

Injection period pressure transient behaviour of two-phase water-oil flow: A semi-analytical study

M.S.M. Althaf, L.J. Hyun*, T.A. Ganat and A.D. Habte

Department of Petroleum Engineering, Universiti Teknologi PETRONAS, Persiaran UTP, 32610 Seri Iskandar, Perak, Malaysia
Phone: +60102958492; Fax: +6053654082

ABSTRACT – This paper presents a study on the pressure transient behaviour during the injection period in a vertical well in the presence of wellbore storage and skin effect. The two-phase water-oil radial flow problem is solved using a semi-analytical technique called the Laplace-Transform Finite-Difference method. Moreover, the factors that influence the degree of wellbore storage and skin effect are analysed. The results demonstrated that the effect of wellbore storage on the pressure transient behaviour is significant during the early times. Factors such as compressibility of fluid, effective wellbore volume and endpoint mobility ratio significantly affect the duration of wellbore storage. The impact of the skin during the injection period is significant on the pressure transient behaviour and could last for a longer duration. A substantial effect of skin is observed for a positive skin factor and unfavourable endpoint mobility ratio. In addition, the duration of the effect is directly proportional to the thickness of the skin zone. Hence attention must be given to the parameters that could prolong these effects and included in the solution methods to precisely interpret the injection period pressure transient behaviour for a better estimation of the reservoir and well properties.

ARTICLE HISTORY

Revised: 29th Jan 2020

Accepted: 8th Feb 2020

KEYWORDS

Injection period;
pressure transient
behaviour;
two-phase;
skin;
wellbore storage.

INTRODUCTION

Well test analysis is a partially controlled field experiment conducted at distinct phases of a reservoir to determine crucial well and reservoir properties that are vital in reservoir description and characterization [1]. Prior to the understanding of the effects of the wellbore conditions on the pressure transient behaviour, well tests were conducted for a longer period of time in order to reach an interpretable behaviour defined by a constant gradient line disregarding the distorted early time behaviour [2]. With time, more interest was shown to study the factors that affect early time pressure data. This led to the understanding that wellbore storage and skin effect are the major wellbore conditions that affect the early time pressure behaviour during a well test [1, 3, 4].

When a well producing for a period of time is shut-in at the surface, the flow from the reservoir does not cease immediately [5]. Similarly, when a well is set for production after a period of shut-in, the initial flow at the surface will be from the fluid within the wellbore with no flow from the formation into the wellbore [6]. This phenomenon of after-flow or unloading is called wellbore storage. Van Everdingen and Hurst [7] were pioneers to highlight the effect of wellbore storage that could cause a contrast between the surface and sandface flow rates as a result of the sudden change in the production rate. Similar to production wells, in an injection well, initially the injected fluid is loaded into the wellbore with no flow into the formation. Eventually, with time, the sandface flow rate will be equal to the surface injection rate with the volume of liquid stored in the wellbore maintained constant [6]. Figure 1 illustrates the difference in surface and sandface flow rates as a result of wellbore storage where the sandface flow rate starting from zero increases exponentially until reaching the surface injection rate with time [8].

The permeability of the formation around the well could vary from the original formation permeability due to the nature of the formation or various operations conducted such as drilling, completion and workover [9]. Van Everdingen [10] analysed the additional pressure drop caused by the resistance of the formation and defined it as the “skin effect”. However, his conception of “thin skin” that adjusts the error between the measured and theoretical bottomhole pressures may be somewhat applicable for a positive skin case under a line-source assumption, yet fails to provide a reasonable explanation in the presence of a negative skin [11]. Instead, the modern-day researchers have accepted the method proposed by Hawkins [12] called “thick skin” to quantify the altered permeability in the damaged zone adjacent to the wellbore using the proposed mathematical relation [13, 14]. This method allows one to alter the permeability of the zone adjacent to the wellbore through a radially composite model to incorporate the skin effect as shown in Figure 2. If the radius of the damaged zone can be estimated, then the permeability in the zone can be determined from a known skin factor using the mathematical relation proposed by Hawkins [12]. Also, through laboratory experiments run on core samples, the depth of the damage can be estimated that allows one to use the thick skin mathematical relation.

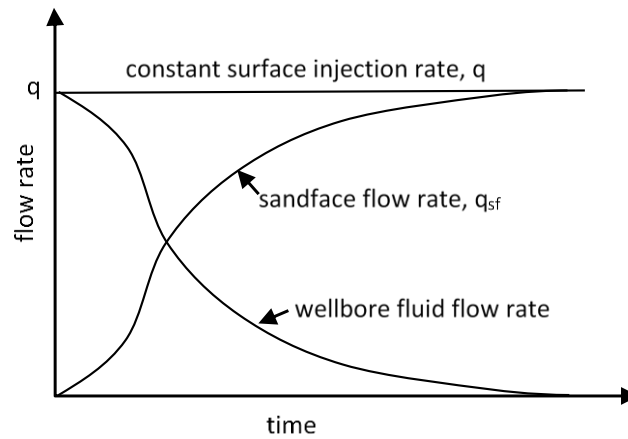


Figure 1. Surface and sandface rates during wellbore storage [6].

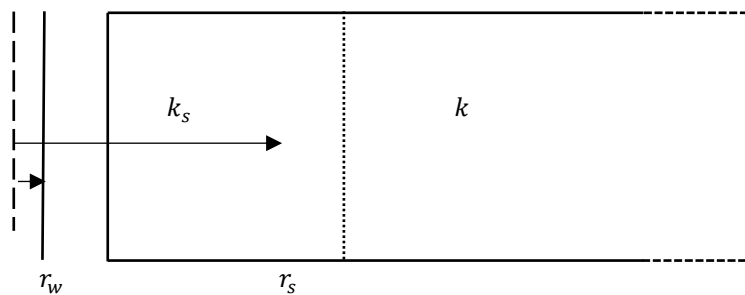


Figure 2. A radially composite model including skin effect.

Unlike the production well tests, the injection well tests are much more complicated due to the distinct properties of the injected and reservoir fluids that result in a two-phase reservoir system with a moving boundary [15]. Also, during injection well tests, the propagations of pressure diffusion and flood front occur in different time scales. During the injection period, the pressure transient behaviour is vastly affected by the propagation of the flood front considering a two-phase water-oil flow [16].

Several studies have been conducted to investigate the effects of wellbore storage and skin on the pressure transient behaviour for a conventional single-phase production well test [6]. However, wellbore storage and skin effect could behave differently during a two-phase water-oil flow as these effects can influence the movement of the flood front in the reservoir during an injection [17]. Hence it is important to investigate the effects of wellbore storage and skin to be able to correctly interpret the pressure transient behaviour during the injection period of a two-phase water-oil flow. Also, understanding the factors that influence wellbore storage and skin effect is vital in the interpretation and running a successful injectivity test.

Most of the recent works that included wellbore storage and/or skin effect in their mathematical models for injectivity test were limited to the validation of the model. Although some of these studies did focus on the sensitivity analysis of the effects of wellbore storage and skin, an extensive study on how certain parameters that influence these effects on the pressure transient behaviour of a two-phase water-oil flow associated during the injectivity test have not been explicitly examined. The primary objectives of this study are (1) to evaluate the effects of skin and wellbore storage on the pressure transient behaviour during the injection of water into an oil reservoir; and (2) to analyse the key factors that affect the duration of wellbore storage and skin effect during the injection period. To solve the two-phase water-oil injection problem, a semi-analytical solution method called the Laplace-transform Finite-difference (LTFD) method is used. This method has proved out to give great approximations and simplify the two-phase water-oil flow associated with the injection of water into the reservoir [13, 17, 18].

MATHEMATICAL MODEL

The model considers injection of water at a constant surface injection rate into a fully penetrating vertical well in a single layer, homogeneous, isothermal and isotropic oil reservoir of uniform thickness that is initially at a constant pressure throughout the reservoir. The overlying and underlying boundaries of the formation are no-flow boundaries. The reservoir and injected fluids are considered slightly compressible with constant viscosities. In constructing the model, the grid blocks in the radial direction are discretized logarithmically as shown in Figure 3.

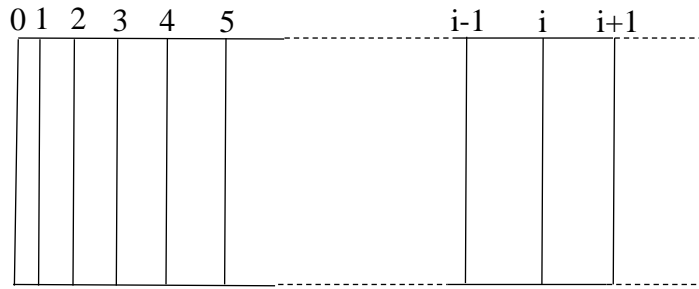


Figure 3. Radially discretized gridding system.

The water-oil flow governed by the two-phase diffusivity equation with known inner boundary condition is solved using the LTFD solution method. In this method, initially, the saturation variation in the reservoir at a given time is determined using the Buckley-Leverett [19] frontal advance formula. The Buckley-Leverett [19] theory is one of the most widely used theory to precisely reflect the movement of the injected water through a porous media [20]. This theory formulated using the law of conservation of mass is even currently used by the recent researchers to precisely model the movement of the interface between the injected water and the reservoir fluid that is replaced by the injected water [21-23]. The usage of the Buckley-Leverett [19] formula allows one to decouple the saturation equation from the pressure equation eliminating the requirement to simultaneously solve the two equations [13, 18]. This approach simplifies the mathematical problem, thereby reduces the computation time required to solve the system of equations.

As injection of water into an oil formation could result in three distinct zones, the flooded zone (water and transition banks) and the unflooded zone (oil bank), the total mobility in these regions vary based on the saturation distribution. It is understood that the saturation variation in the radial direction before the flood front ($r_w < r < r_f$) behaves as per Buckley-Leverett [19] equation whereas ahead of the flood front ($r > r_f$), the saturation remains constant at irreducible water saturation S_{wi} . Hence, for the two-phase water-oil flow, the total mobility λ_t at a given time t and radial distance r is defined as,

$$\lambda_t(r, t) = k(r) \left[\frac{k_{rw}(r, t)}{\mu_w} + \frac{k_{ro}(r, t)}{\mu_o} \right], r_w < r < r_f \tag{1}$$

where k is the absolute permeability of the reservoir, k_{rw} is the relative permeability of water, k_{ro} is the relative permeability of oil, μ_w is the viscosity of water and μ_o is the viscosity of oil.

Beyond the flood front, the total mobility is equal to the endpoint mobility of oil. With known saturation and mobility distribution in the reservoir, the transmissibility and accumulation terms can be determined for a given time to solve the inner boundary condition for the innermost grid block ($i = 0 = r_w$) and the two-phase diffusivity equation for the other grid blocks ($i \geq 1$). The two-phase radial diffusivity equation, a PDE for pressure P with respect to time t and radius r that governs the water-oil flow given by Eq. (2) is used to obtain the pressure profile.

$$\frac{1}{r} \frac{\partial}{\partial r} \left(\lambda_t r \frac{\partial P}{\partial r} \right) = \frac{\phi c_t}{0.0002637} \frac{\partial P}{\partial t} \tag{2}$$

where c_t is the total compressibility and ϕ is the porosity of the formation.

Although the model assumes constant fluid compressibility, it accounts for the change in the total compressibility of the system at different locations of the reservoir at a given time based on the saturation distribution. The total compressibility c_t at different grid points is determined using Eq. (3).

$$c_t(r, t) = S_w(r, t) c_w + [1 - S_w(r, t)] c_o + c_f \tag{3}$$

where S_w is the water saturation, c_w is the compressibility of the injected water, c_o is the compressibility of the reservoir fluid (oil) and c_f is the compressibility of the formation.

The effects of wellbore storage and skin are introduced into the inner boundary condition set at the grid boundary $i = 0$. Although there can be variable wellbore storage and skin effect based on changing injection/production rates, a constant skin and wellbore storage under a constant surface injection rate are considered [11, 24, 25]. The effects of wellbore storage and skin are incorporated into the model by modifying the inner boundary condition. The wellbore storage effect is incorporated mathematically into the inner boundary condition by considering the difference between the surface injection rate and the sandface flow rate using a mass balance for the wellbore [24]. Equation (4) has been previously used to model the wellbore storage effect [18]. This mathematical relation accurately produces the effect of wellbore

storage as shown in Figure 1 where the sandface rate q_{sf} starts from zero and reaches the surface injection rate q with time t . Considering a constant water formation volume factor B_w , the sandface injection rate q_{sf} is given by,

$$q_{sf} = q + \frac{24}{B_w} C \frac{dP_w}{dt} \tag{4}$$

where P_w denotes the bottomhole pressure during the injection and C is the wellbore storage coefficient.

The wellbore storage coefficient C can be defined in different ways. In this case, since injection of water into the well results in a single phase inside the wellbore that causes the effect, the wellbore storage coefficient C is defined as a product of the effective wellbore volume V and the compressibility of the injected water inside the wellbore c_w .

$$C = Vc_w \tag{5}$$

In the presence of skin, the sandface flow rate of the injected water is open to the reservoir formation of thickness h with an altered permeability of k_s in the skin zone. Hence, the sandface flow rate q_{sf} is given by Darcy’s law as,

$$q_{sf} = \frac{k_s k_{rw,max} h}{141.2 B_w \mu_w} \left(r \frac{\partial P}{\partial r} \right)_{r=r_w} \tag{6}$$

where $k_{rw,max}$ is the maximum relative permeability of water. The product of the absolute permeability of the formation around the wellbore and the maximum relative permeability of water provides the effective permeability of the injected water open to flow into the formation from the wellbore during a two-phase flow.

The inner boundary condition for two-phase water-oil flow with the inclusion of wellbore storage by altering the surface injection rate with the sandface flow rate into the formation adjacent to the wellbore of permeability of k , or in the presence of skin, permeability of k_s , is given in Eq. (7). The inner boundary condition remains the same for all different definitions of the wellbore storage coefficient.

$$q = \frac{k_s k_{rw,max}}{141.2 B_w \mu_w} \left(r \frac{\partial P}{\partial r} \right)_{r=r_w} - \left(\frac{24}{B_w} C \frac{dP_w}{dt} \right) \tag{7}$$

Although the inner boundary condition consists of the skin effect with the addition of the altered permeability term to which the radial flow is open to at the beginning, the permeability of the skin zone must be assigned. In this model, whenever the skin factor takes a value other than zero, the “thick skin” mathematical relation is used as given in Eq. (8) to quantify the formation damage to determine the altered permeability of the skin zone since it allows one to compute for both, positive and negative skin effects [12]. Based on the mathematical relation, the reservoir is divided into two composite zones as shown in Figure 2 where the zone between the wellbore radius r_w and the skin radius r_s possesses the altered permeability value k_s due to presence of skin S while the formation beyond the skin radius possesses the original reservoir permeability k . A positive skin would result in the permeability of the skin zone to be lesser than the rest of the formation, a negative skin would cause the permeability of the skin zone to be higher than that in the formation while a zero skin would yield a permeability value equal to that of the original permeability of the formation [14].

$$S = \left(\frac{k}{k_s} - 1 \right) \ln \left(\frac{r_s}{r_w} \right) \tag{8}$$

The inner boundary condition given by Eq. (7) and the radial diffusivity equation given by Eq. (2) are PDEs with time and space fractional derivatives. Hence, in solving the system of equations using the LTFD method, initially, Laplace transformation is applied to remove the time domain. This eliminates the necessity for the application of time discretization thereby resolving the instability issues while solving the moving boundary problem. Then the equations in Laplace space are approximated using Finite difference method to solve the spatial domain. Later the results are numerically inverted back to real-time from Laplace space using Stehfest [26] algorithm. A detailed description of the LTFD solution method to solve the two-phase injection problem is given in [18]. The mathematical model is computed on MATLAB R2017a software. An evaluation of the number of grids performed similar to the approach used by Bouaffane and Talbi [27] showed that the increase in the number of grids more than 800 resulted in an increased computational time with no improvement in the accuracy of the results. As such, the gridblocks in the model are logarithmically discretised into 800 segments in the radial direction.

Pressure derivative is the primary tool used in well test to precisely interpret the pressure transient data [28]. As the injection period problem is complicated, the conventional arithmetic derivative may yield significant noise due to mathematical issues [28, 29]. Hence choosing an appropriate algorithm to determine the pressure derivative is very crucial in interpreting a two-phase water-oil injectivity problem. As such, here, a three- smoothed point algorithm given by Eq.

(9) similar to that proposed by Bourdet et al. [30] to determine the pressure derivative with respect to the natural logarithm of time is used.

$$\frac{\partial p}{\partial \ln t_i} = \left[\frac{\ln\left(\frac{t_i}{t_{i-k}}\right) \Delta p_{i+j}}{\ln\left(\frac{t_{i+j}}{t_i}\right) \ln\left(\frac{t_{i+j}}{t_{i-k}}\right)} + \frac{\ln\left(\frac{t_{i+j} t_{i-k}}{t_i^2}\right) \Delta p_i}{\ln\left(\frac{t_{i+j}}{t_i}\right) \ln\left(\frac{t_i}{t_{i-k}}\right)} + \frac{\ln\left(\frac{t_{i+j}}{t_i}\right) \Delta p_{i-k}}{\ln\left(\frac{t_i}{t_{i-k}}\right) \ln\left(\frac{t_{i+j}}{t_{i-k}}\right)} \right] \tag{9}$$

where,

$$\ln(t_{i+j}/t_i) = \ln t_{i+j} - \ln t_i \geq 0.2 \tag{10}$$

$$\ln(t_i/t_{i-k}) = \ln t_i - \ln t_{i-k} \geq 0.2 \tag{11}$$

The analysis is performed for both, favourable ($M \leq 1.0$) and unfavourable ($M > 1.0$) endpoint mobility ratios. The endpoint mobility ratio M for two-phase water-oil flow is defined as,

$$M = \frac{k_{rw,max}/\mu_w}{k_{ro,max}/\mu_o} = \frac{\lambda_w}{\lambda_o} \tag{12}$$

where $k_{ro,max}$ is the maximum relative permeability of oil, λ_w is the endpoint mobility of water and λ_o is the endpoint mobility of oil.

RESULTS AND DISCUSSION

Initially, the LTFD model is validated for the base case by comparing the change in pressure ($\Delta P = P_{wf} - P_i$) and the pressure derivative ($\Delta P'$) determined using Eq. (9) during the injection period by comparing the results obtained from ECLIPSE 100, a commercial numerical simulator. ECLIPSE 100, the Schlumberger reservoir simulation software solves the black oil system of equations numerically on corner-point grids [31]. The input data used for the base case of the analysis is given in Table 1. For all the cases considered, except for the parameters that have been altered, the remaining parameters are kept the same as in the base case.

Table 1. Input data for the base case.

Parameter	Value
Porosity, ϕ , fraction	0.30
Permeability, k , mD	2500
Initial reservoir pressure, P_i , psi	4000
Oil formation volume factor, B_o , rb/scf	1.00
Water formation volume factor, B_w , rb/scf	1.00
Wellbore radius, r_w , ft	0.35
Compressibility of oil, c_o , psi ⁻¹	8×10^{-6}
Compressibility of water, c_w , psi ⁻¹	3×10^{-6}
Compressibility of rock, c_r , psi ⁻¹	6×10^{-6}
Irreducible water saturation, S_{wi} , fraction	0.25
Residual oil saturation, S_{or} , fraction	0.2
Formation thickness, h , ft	100
Maximum relative permeability of water, $k_{rw,max}$ (at S_{or})	0.3
Maximum relative permeability of oil, $k_{ro,max}$ (at S_{wi})	0.8
Water viscosity, μ_w , cP	0.6
Surface injection rate, q_w , bbl/day	700
Injection period, t , hrs	100

Figure 4 shows the pressure transient behaviour during the injection period computed using the input data given in Table 1 for favourable ($M = 0.625$) and unfavourable ($M = 3.0$) endpoint mobility ratios using the LTFD model and ECLIPSE 100. For this base case, no wellbore storage and skin effect are taken into account. The change in pressure ΔP and the pressure derivative $\Delta P'$ curves obtained from the LTFD model and ECLIPSE 100 agreed excellently. Only an

insignificant difference of less than 1% was observed in the results between the models at the early times. However, results from the later times showed little or no differences at all.

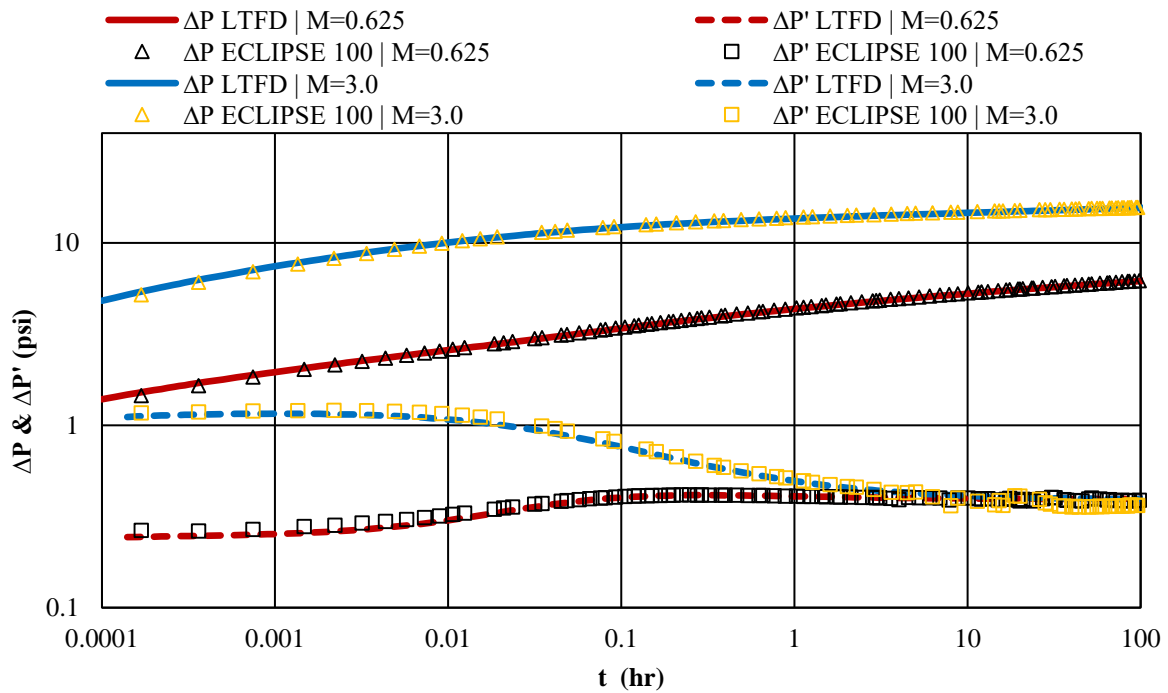


Figure 4. Comparison of ΔP and $\Delta P'$ results for the base case from the LTFD model and ECLIPSE 100.

The results suggest that the injection period pressure response is highly affected by the movement of the flood front as explained by the researchers in this area [16]. However, the movement of the flood front for two-phase water-oil flow is highly influenced by the endpoint mobility ratios. Initially, the formation around the wellbore is filled with oil. As such, the pressure derivative curve at very early times reflects the initial condition around the wellbore filled with the reservoir fluid. With time, as the injection proceeds, the oil from the near-wellbore region is displaced and replaced by the injected water. Once the oil from the region adjacent to the wellbore is completely replaced by the injected water, the pressure derivative value converges at a single value determined using the endpoint mobility ratio of water.

In comparison with the base case, the effects of wellbore storage and skin are analysed to study their influence on the pressure behaviour during the injection period using the LTFD model. Listed below are the identified key parameters that are analysed to study their influence on wellbore storage and skin effect on the injection period pressure transient behaviour.

Wellbore Storage

The effect of wellbore storage primarily depends on the duration of the sandface flow rate to eventually equalize the surface injection rate. Here, the main parameters that affect the wellbore storage as listed in Table 2 are analysed. Based on the definition of the wellbore storage coefficient, the factors that affect the duration may vary. However, the wellbore storage during a water injection problem is due to the presence of a single phase in the wellbore. As such, the model considers a wellbore storage coefficient as defined in Eq. (5).

Table 2. Parameters analysed during each case.

Wellbore storage	Skin
1-Endpoint mobility ratio	4-Endpoint mobility ratio
2-Compressibility of fluid	5-Altered permeability
3-Effective wellbore volume	6-Skin radius

Case 1: Endpoint mobility ratio

In case 1, the effect of the endpoint mobility ratio on wellbore storage is analysed by considering two cases of favourable ($M \leq 1$) and unfavourable ($M > 1$) endpoint mobility ratios as shown in Table 3, while maintaining a constant effective wellbore volume of 8000 ft^3 , fixed compressibility values, thereby maintaining a constant wellbore storage coefficient of $C = 4.27 \times 10^{-3} \text{ bbl/psi}$.

Table 3. Viscosity and corresponding endpoint mobility ratios.

μ_0 (cP)	M
1.0	0.625
4.8	3.0

Figure 5 shows the comparison of the change in pressure and its derivative results for the two scenarios considered. Although the end of the wellbore storage effect is not precisely when the pressure transient behaviour starts to act in the absence of the effect, it is a good approximation to make that the effect completely ceases once the pressure transient behaviour starts to respond as in the base case in which neither wellbore storage nor skin is taken into account. Here t_1 and t_2 are the times at which the wellbore storage completely cease for favourable and unfavourable endpoint mobility ratio scenarios respectively. It is evident that the effect is significant for an unfavourable endpoint mobility ratio that results in a longer unit slope line, higher peak value and a longer duration of the effect ($t_2 > t_1$). Although the endpoint mobility ratio does not affect the quantity of the wellbore storage coefficient, it does affect the propagation of the front within the reservoir.

For a favourable endpoint mobility ratio where $M \leq 1$, the oil is able to propagate with a velocity equal to, or greater than that of the injected water [20]. This condition results in no propensity for the injected water to by-pass the reservoir fluid which results in a piston-like displacement. Hence the propagation of the injected water into the reservoir becomes rather simple resulting in consuming a shorter time to completely fill the wellbore with the injected fluid to equalize the surface and sandface injection rates. A non-ideal displacement that occurs in an unfavourable endpoint mobility ratio system where $M > 1$ is more common in nature [20]. Here, the injected water is capable of propagating rapidly than the reservoir fluid. This results in disturbed saturation profiles due to viscous fingering and tongues as the high mobility water by-passes the lower mobility oil in the reservoir [32]. Hence, the injected water is lost into the formation at a higher rate. This unfavourable movement of the water and the front results in consuming more time for the injected water to completely fill in the wellbore, thereby resulting in a delay for the surface injection rate to be equivalent with the sandface flow rate. As such, the wellbore storage effect could last longer when injecting water into a reservoir containing heavier oil. This could also result in an early breakthrough of water into production [33].

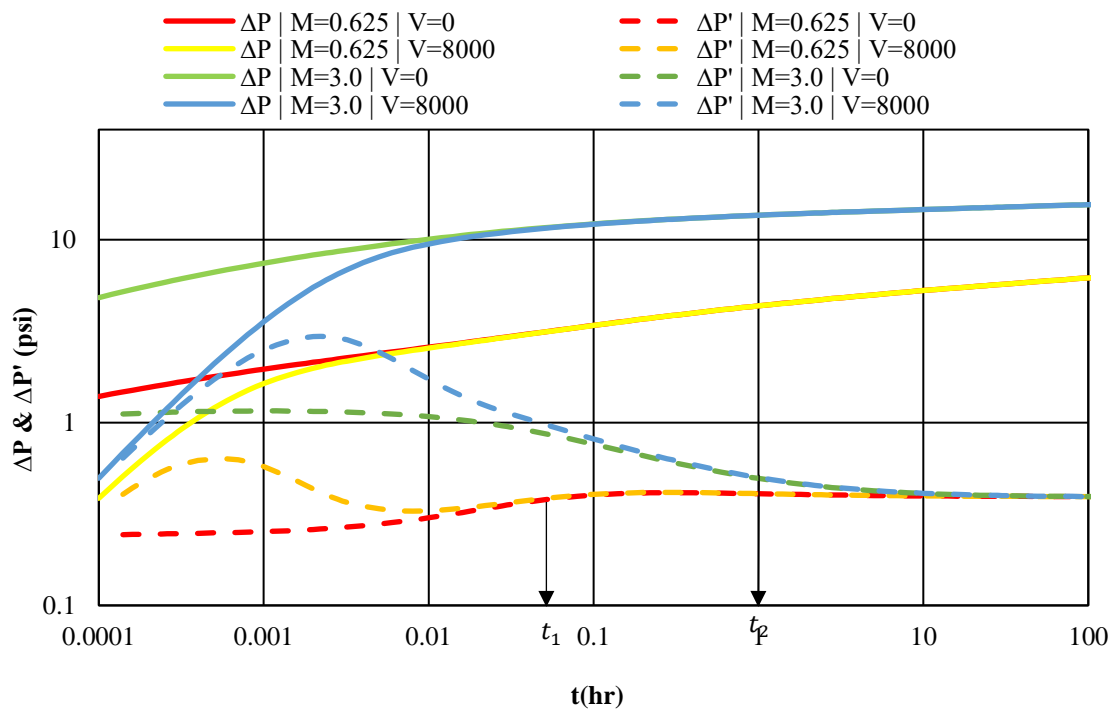


Figure 5. ΔP and $\Delta P'$ for Case 1.

Case 2: Effective wellbore volume

To analyse the influence of the effective wellbore volumes on wellbore storage, a range of effective wellbore volumes while maintaining constant compressibility as in the base case for an unfavourable endpoint mobility ratio $M = 3.0$ are chosen. Table 4 shows the effective wellbore volumes considered for the analysis and the corresponding wellbore storage coefficient values calculated using Eq. (5).

Table 4. Effective wellbore volumes and corresponding wellbore storage coefficient values for Case 2.

$V (ft^3)$	$C(bbl/psi)$
0	0
4000	2.14×10^{-3}
8000	4.27×10^{-3}
12000	6.41×10^{-3}

Figure 6 shows the influence of the effective wellbore volume on pressure behaviour during the injection period. The effective wellbore volume is directly proportional to the coefficient of wellbore storage. As such, an increase in the effective wellbore volume results in an increase in the coefficient of wellbore storage as shown in Table 4. Comparison of the results with the base case suggests that the increase in the effective wellbore volume results in a longer duration of the effect as denoted by $t_3 (V = 4000 ft^3)$, $t_4 (V = 8000 ft^3)$ and $t_5 (V = 12000 ft^3)$ that represent the time taken for the surface injection rate to match the sandface flow rate for each scenario considered ($t_5 > t_4 > t_3$). As the value gets higher, a longer unit slope line and a shift in the peak value is encountered. This trend is very similar to that obtained by Li et al. [17] when analysing the variation in shapes of the pressure derivative curve in the presence of wellbore storage during an injection well test.

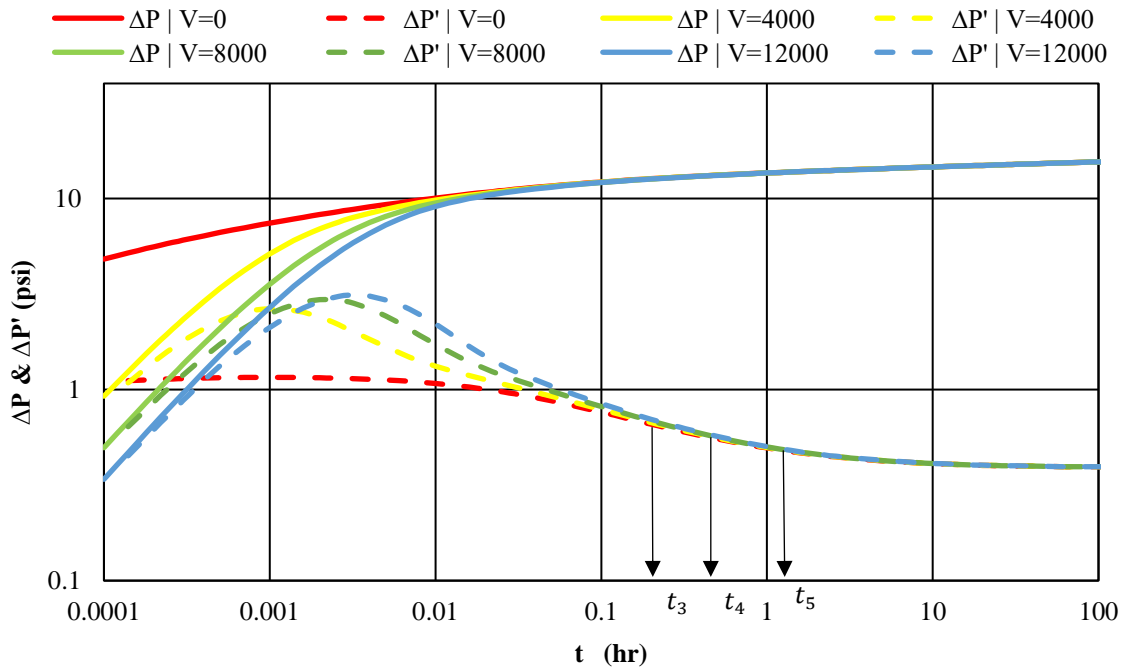


Figure 6. ΔP and $\Delta P'$ for Case 2.

As the effective wellbore volume increases, the amount of fluid the wellbore can accommodate increases thereby resulting in an increased time to completely fill in the wellbore under a constant surface injection rate. This is also another reason why the effect lasts longer for a horizontal well as the effective wellbore volume is higher than a vertical well due to the presence of both, vertical and horizontal well trajectories [34]. Opening or shutting a well can be performed using the main valve on the Christmas tree or a downhole valve installed in the completion assembly. In a production well test, shutting the well using a downhole valve will minimize the duration of the effect by reducing the effective wellbore volume [5]. However, this operation is not possible in an injection well as the water is injected into the well at the surface. The injected water initially fills the wellbore with little or no flow into the formation. As such, the wellbore storage effect due to the effective wellbore volume during the injection period is almost unavoidable.

Case 3: Compressibility of fluids

Compressibility is defined as the change in volume per unit change in the prevailing pressure [35]. The effect of the compressibility of fluids on wellbore storage is studied by selecting a range of compressibility values for the injected fluid while maintaining a constant effective wellbore volume of 8000 ft³ for an endpoint mobility ratio $M = 3.0$. The compressibility values were chosen on the typical range magnitude for water that is usually in the order of 10^{-6} psi⁻¹ [36]. Table 5 shows the chosen water compressibility values and the corresponding wellbore storage coefficient values for the scenarios considered.

Table 5. Fluid compressibility values and corresponding wellbore storage coefficient for Case 3.

c_w (psi ⁻¹)	C (bbl/psi)
0.5×10^{-6}	7.12×10^{-4}
1.0×10^{-6}	1.42×10^{-3}
4.0×10^{-6}	5.7×10^{-3}
8.0×10^{-6}	1.14×10^{-2}

Figure 7 shows the influence of the compressibility of the injected fluid in the presence of wellbore storage on pressure behaviour during the injection period.

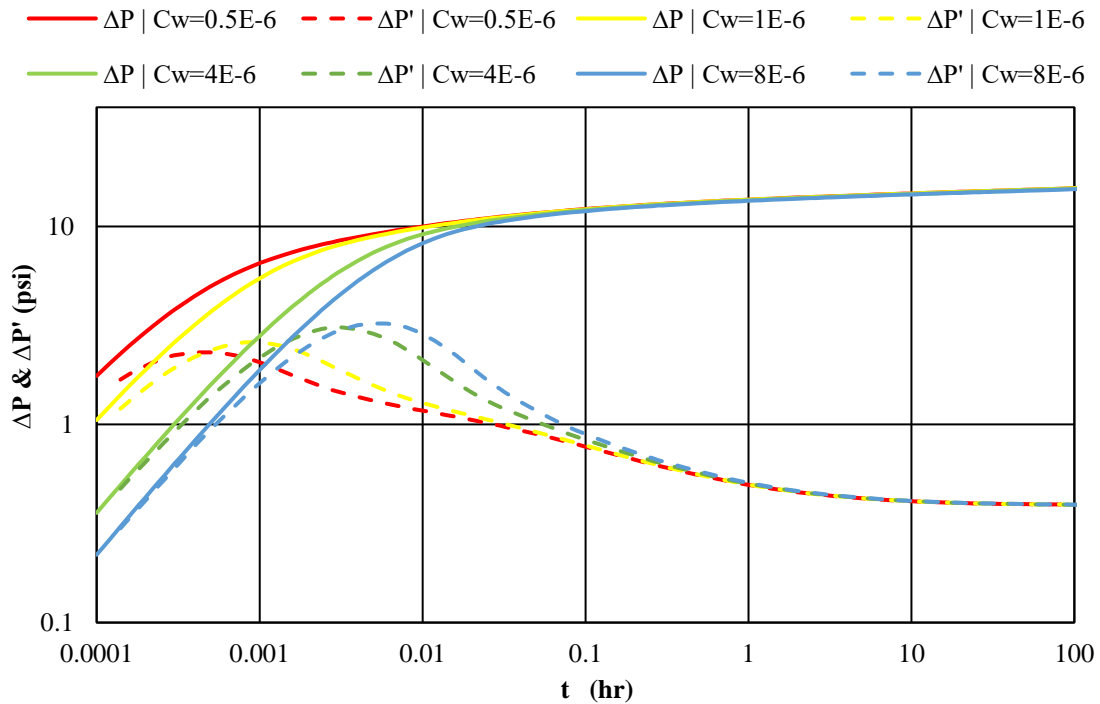


Figure 7. ΔP and $\Delta P'$ for Case 3.

The compressibility of the fluid in the wellbore, which is typically the injected fluid in an injection well, is directly proportional to the coefficient of wellbore storage. Similar to the results obtained for the previous case of effective wellbore volume, Figure 7 shows that the increase in the injected fluid compressibility develops a longer unit slope line and a shift in the peak value to the right of the pressure derivative curve. Hence, the increase in the compressibility of the fluid within the wellbore results in an increase in the duration of the effect. This is mainly due to the slightly compressible nature of the fluid that results in marginal compaction in the fluid in the wellbore as the pressure in the bottomhole increases during the injection. This compaction results in consuming more time for the wellbore to be completely filled with the injected fluid to result in equal surface and sandface injection rates. However, the variation in compressibility of the injected water due to the increase in pressure is lower as the compressibility of water is a weak function of pressure [37]. Consequently, during an injection well test, the effect of wellbore storage can be minimized by injecting water with higher salinity as the water compressibility decreases with increasing salinity [38]. Not only does the increment in salinity of the injected water reduces the effect of wellbore storage, but also increases the oil recovery [39]. Although not shown here, the compressibility of the reservoir fluid had insignificant effects on wellbore storage during a two-phase water-oil flow.

The wellbore storage in a conventional production well test is caused due to the storage or after-flow of oil in the wellbore that has fluid compressibility in the range of $5 \times 10^{-6} \text{ psi}^{-1}$ to $12 \times 10^{-6} \text{ psi}^{-1}$ [36]. This is slightly higher than that of the compressibility of water. As such, the duration of wellbore storage during a production test might last longer than the injection well test. This also supports the findings in gas well testing suggesting that the injection of gas into a well could result in significant wellbore storage effect as the gas compressibility is much higher compared to the compressibility of oil or water [40, 41]. Also, below the bubble point pressure P_b , the variation in oil compressibility is fairly high due to the liberation of the dissolved gases from the reservoir fluid with decreasing reservoir pressure that could result in consequential wellbore storage effect during a production well test [42]. Figure 8 shows the variation of the oil compressibility with pressure.

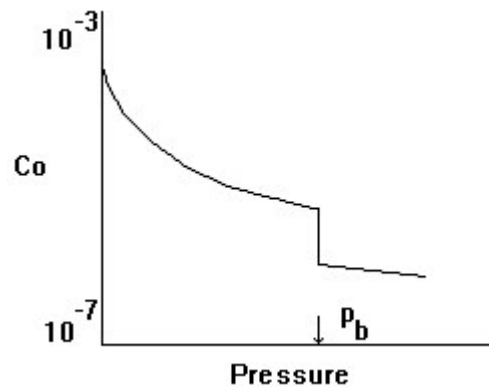


Figure 8. Variation of oil compressibility with pressure [37].

In a conventional production welltest, the duration of wellbore storage is influenced by the effective wellbore volume, fluid compressibility and the formation permeability [43]. However, in an injection well test, besides the effective wellbore volume and fluid compressibility, the endpoint mobility ratio affects the duration of the wellbore storage as the injection period pressure transient behaviour is vastly affected by the mobility of the two-phases in the reservoir. As the change in the injection rate could also result in varying wellbore storage effect, maintaining a constant surface injection rate is extremely important in avoiding the influence of wellbore storage on the pressure transient behaviour throughout the test.

Skin effect

The skin effect is analysed by altering the formation permeability to k_s adjacent to the wellbore until the skin radius r_s , using the Hawkins [12] formula. Here, the main parameters that affect the pressure transient behaviour during the injection period in the presence of skin effect as listed in Table 2 are analysed.

Case 4: Endpoint mobility ratio

To analyse the effect of the endpoint mobility ratios on skin effect, a positive skin factor of $S = 3$ with a skin radius of $r_s = 2.1416 \text{ ft}$ that would result in an altered permeability of $k_s = 942.2 \text{ mD}$ in the damaged formation is considered. Figure 9 shows the pressure transient results for favourable and unfavourable endpoint mobility ratios in the presence of a positive skin factor. It is evident that the pressure derivative curve shows a higher degree of variation resulting in negative pressure derivative values as the front approaches the skin radius for an unfavourable endpoint mobility ratio in the presence of a positive skin factor. A similar trend was observed by Boughrara [16] in her studies when comparing the synthesized analytical model with the simulator results in the presence of a positive skin factor of $S = 14.9$. However, the high degree of variation in the pressure derivative curve is not only due to the high skin, but also due to the high endpoint mobility ratio. For both cases, after the front has propagated beyond the skin radius, the pressure derivative curve starts to behave the same as the zero-skin case reflecting the response from the formation with the original permeability. However, it is noticeable that the time taken for the favourable mobility ratio (t_o) to obtain the response from the undamaged zone is shorter than the unfavourable endpoint mobility ratio scenario. Here the unfavourable endpoint mobility ratio scenario is yet to receive the response from the zero-skin zone and might require a longer injection period for that purpose.

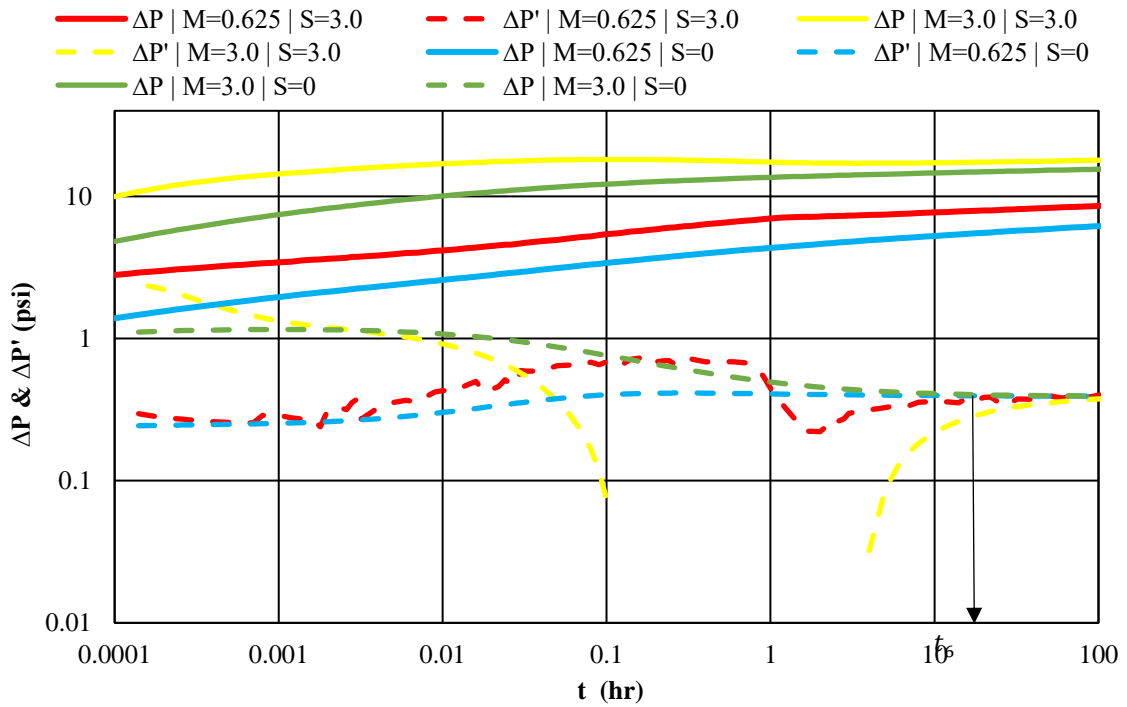


Figure 9. ΔP and $\Delta P'$ for Case 4.

This adverse variation in the pressure derivative curve for an unfavourable endpoint mobility ratio occurs due to the unfavourable displacement of the injected water in the reservoir. The ability of the high mobility water to by-pass the lower mobility reservoir fluid would cause a delay in displacing all the oil from the near-wellbore region. However, for a favourable endpoint mobility ratio, the oil from the skin zone is swept easily in a piston-like displacement causing the front to propagate much easier. Hence, the oil from the near-wellbore region is completely swept by water much faster causing the front to escape the skin-zone earlier in comparison to the unfavourable endpoint mobility ratio scenario. As such, the effect of skin could last for a significantly longer period of time in a reservoir containing heavier oil. A combination of severe skin and heavier oil would result in a drastic delay in receiving the desired response from the unaffected zone.

Case 5: Skin factor or altered permeability

As it was identified previously that the skin effect is significant for an unfavourable endpoint mobility ratio, the effect of the degree of skin that causes the change in permeability of the skin zone is analysed for an unfavourable endpoint mobility ratio. Both, positive and negative skin factors are considered. Table 6 gives the altered permeability of the skin zone calculated based on the skin factor and skin radius of $r_s = 2.1416 \text{ ft}$ using Eq. (8). The injection period is extended to 200 hours.

Table 6. Skin factor values and the corresponding altered permeability values for Case 5.

S	$k_s(mD)$
5.0	664.8
0	2500 (original permeability)
-1.5	14543.3

A positive skin causes a reduction in the permeability and a negative skin value results in an increase in the permeability of the skin zone. From the results shown in Figure 10, it is noticeable that the effect of skin on the pressure transient behaviour is significant for a positive skin factor. Also, the skin effect lasts longer for positive skin as it is yet to obtain a response from the zero-skin zone. The delay in receiving the response from the zero-skin zone in the presence of a positive skin is due to the reduced permeability in the skin zone that hinders the movement of the front. On the other hand, the time taken for the negative skin factor scenario (t_7) is lesser as it enables the front to propagate much faster through the increased permeability in the skin zone causing the front to move out of the skin zone faster. This scenario is highlighted by Habte and Onur [18] that disallowed them to obtain the desired pressure derivative value at the beginning replicating the initial condition around the wellbore due to the rapid motion of the injected water in the presence of a negative skin factor. This relation can be clearly explained with the support of Darcy’s law equation given by Eq. 6 where

the flow rate is directly proportional to the permeability of the formation. Also, it is worthwhile mentioning that the injection of water could result in stimulating or damaging the formation further. Injection of water into a formation with water-sensitive clays could further aggravate the problem due to clay swelling that could result in smaller throats causing a reduction in the permeability [44]. Injection of water into a water-compatible reservoir could increase the permeability as the fine sand particles are migrated away from the near-wellbore region [45].

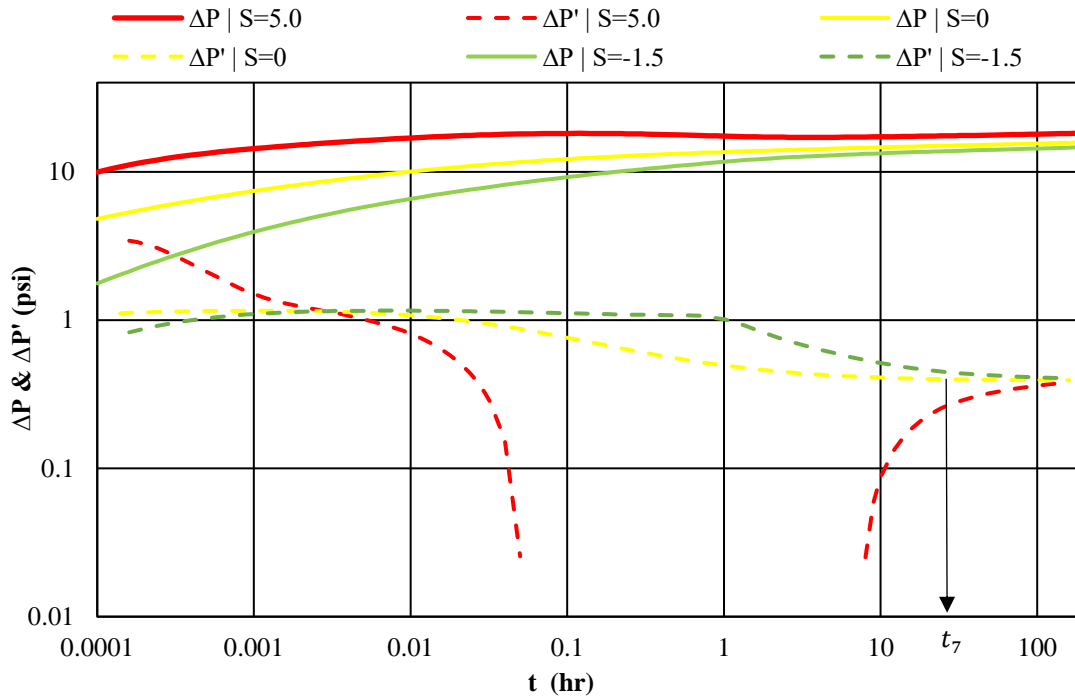


Figure 10. ΔP and $\Delta P'$ for Case 5.

Case 6: Skin radius

The “skin zone”, the region of altered permeability could extend from a few inches from the wellbore to several feet into the formation [46]. Hence, the effect of the skin radius on the pressure transient behaviour during the injection period is analysed by considering various thicknesses of the skin zone while maintaining the same permeability in the damaged zone as summarized in Table 7. The analysis is performed for an unfavourable endpoint mobility ratio of $M = 3.0$.

Table 7. Skin factor corresponding to assigned permeability and skin radius for Case 6.

k_s (mD)	r_s (ft)	S
664.8	1.18	3.35
664.8	2.14	5
664.8	3.71	6.52
2500	0	0

The comparison of the results for the scenarios considered as seen in Figure 9 suggests that the skin effect lasts longer for a thicker skin zone. As the movement of the front vastly affects the injection period pressure behaviour, the effect of skin would last until the front moves outside the skin zone. Although the pressure derivative curves show a similar trend at the early time due to the same permeability in the region, as the thickness of the zones vary, the flood front in the scenario with the least skin radius is able to receive the response from the zero-skin region sooner than the scenarios with a higher skin radius. As such, the time spent by the flood front in the skin zone is directly proportional to the thickness of the skin zone. However, it is understood that the time spent by the flood front in the skin zone also depends on the endpoint mobility ratio and the skin factor as the flood front is able to propagate much faster in a favourable endpoint mobility ratio system with a negative skin factor.

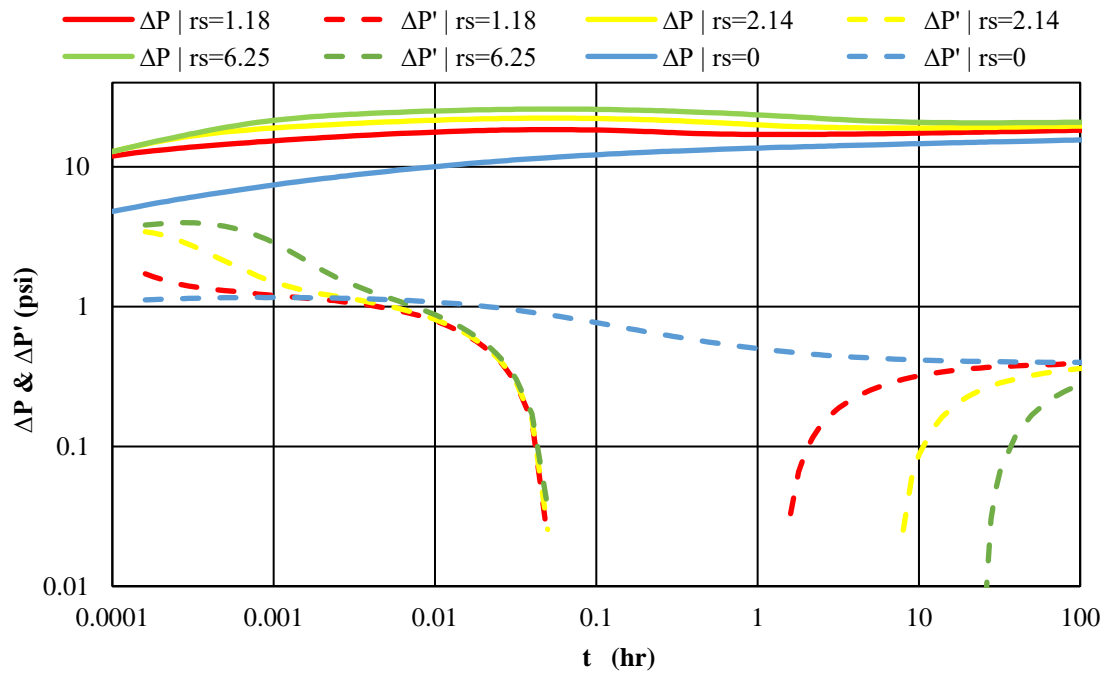


Figure 11. ΔP and $\Delta P'$ for case 6.

In a conventional production well test, the presence of skin only distorts the early time region of the pressure transient data [6]. However, that is not the case in an injection well test. For cases 4-6 in which the effect of skin is included, the time taken to receive the pressure response from the zone beyond the skin region is significantly high. As the movement of the front mainly affects the injection period pressure behaviour, the total time taken to completely displace the reservoir fluid from the near-wellbore region, formed water front to eventually propagate and move outside the skin zone could take a significantly long time. Certain scenarios are yet to receive the response from the zero-skin zone despite having an injection period of 100 hours as the water front is yet propagate beyond the skin radius proves the adverse effect of the presence of skin on the interpretation of the pressure response during an injectivity test. The effect of skin on the pressure transient behaviour can be minimized by performing well stimulation on injection wells to maximize the injection rates and conducting preliminary studies on the quality and incompatibilities of the injected water to avoid clay swelling or deposition of scale that might result in blocking the pore throats [47]. Although these actions cannot alter the endpoint mobility ratio of the system, the changes in the degree of skin and skin radius can still minimize the duration of the effects on the pressure behaviour. However, the injection of hot water reduces the viscosity of the reservoir fluid, thereby reducing the endpoint mobility ratio of the system around the wellbore [48].

CONCLUSION

Unlike the conventional well test interpretations where the effects of skin and wellbore storage only affect the early time pressure data, for a two-phase water-oil injection problem, these effects behave differently as the movement of the flood primarily influences the injection period pressure behaviour. The wellbore storage effect although distorts only the early-time region, it could impair the pressure response from zone adjacent to the wellbore restricting one to determine the near-wellbore conditions such as fractures, coning and thin skin. Effective wellbore volume and compressibility of the fluid within the wellbore influence the amount of wellbore storage. Although the endpoint mobility ratio does not influence the coefficient of wellbore storage whatsoever, it does significantly affect the duration of the effect. The effect of skin can be consequential on the injection period pressure behaviour. The skin effect could last for a significantly longer period of time until the front reaches the skin radius to obtain the pressure response from the region beyond the skin zone. The factors that contribute in restricting the movement of the front adversely affect the pressure transient behaviour. Reduced permeability and/or larger skin radius result in the effect lasting for a longer period. Both, wellbore storage and skin effect are significant for an unfavourable endpoint mobility ratio. If these factors are not taken into account, the aims from the well test can only be achieved after the effects of wellbore storage and skin cease that can last for a significant period of time resulting in an inefficient well test. Hence, it is important to fully understand the effects of these parameters on the pressure transient behaviour during an injection well test to distinguish the interpretable reservoir response and extract information from the early time pressure data.

ACKNOWLEDGEMENTS

The authors would like to thank Universiti Teknologi PETRONAS for the unconditional support throughout the course of study. Many thanks to the editorial board and the reviewers of the Journal of Mechanical Engineering and Sciences for their critical review and valuable inputs in improving the manuscript.

REFERENCES

- [1] F. J. Kuchuk, M. Onur, and F. Hollaender, *Pressure transient formation and well testing: convolution, deconvolution and nonlinear estimation vol. 57*: Elsevier, 2010.
- [2] H. J. Ramey Jr, "Short-Time Well Test Data Interpretation in the Presence of Skin Effect and Wellbore Storage," presented at SPE 39th Annual California Regional Fall Meeting held In Bakersfield : Journal of Petroleum Technology, 1970.
- [3] A. C. Gringarten, D. Bourdet, P. A. Landel, and V. J. Kniazeff, "A Comparison Between Different Skin and Wellbore Storage Type-Curve for Early-Time Transient Analysis," presented at the 54th Annual fall Technical Conference and Exhibition of the Society of Petroleum Engineers of AIME, 1979.
- [4] K. Razminia, A. Hashemi, A. Razminia, and D. Baleanu, "Explicit deconvolution of well test data dominated by wellbore storage," in *Abstract and Applied Analysis*, 2014.
- [5] P. Donnez, *Essentials of Reservoir Engineering vol. 2*. Paris, France: Editions Technip, 2012.
- [6] J. Lee, J. B. Rollins, and J. P. Spivey, *Pressure Transient Testing vol. 9*, 2003.
- [7] A. F. Van Everdingen and W. Hurst, "The Application of the Laplace Transformation to Flow Problems in Reservoirs," *Petroleum Transactions, AIME*, pp. 305-324-B, 1949.
- [8] D. G. Hatzignatiou, A. M. M. Peres, and A. C. Reynolds, "Effect of Wellbore Storage on the Analysis of Multiphase Flow Pressure Data," *SPE Formation Evaluation*, vol. 9, pp. 219-227, 2013.
- [9] L. P. Dake, *The practice of reservoir engineering (revised edition) vol. 36*: Elsevier, 2001.
- [10] A. Van Everdingen, "The skin effect and its influence on the productive capacity of a well," *Journal of petroleum technology*, vol. 5, pp. 171-176, 1953.
- [11] P. Liu, W. Li, J. Xia, Y. Jiao, and A. Bie, "Derivation and application of mathematical model for well test analysis with variable skin factor in hydrocarbon reservoirs," *AIP Advances*, vol. 6, p. 065324, 2016.
- [12] M. F. J. Hawkins, "A Note on the Skin Effect," *Journal of Petroleum Technology*, 1956.
- [13] A. D. Habte, "Laplace - Transform Finite Difference and Quasistationary Solution Method for Two - And Three Phase Injection/Falloff test," PhD dissertation, Universiti Teknologi Petronas, Bandar Seri Iskandar, Perak, Malaysia, 2017.
- [14] S. Koščak Kolin, T. Kurevija, and D. Grebenar, "Pressure build-up test analysis of the reservoir system with the multiphase flow," *Rudarsko-geološko-naftni zbornik*, vol. 33, pp. 75-84, 2018.
- [15] D. Bourdet, *Well Test Analysis : The Use of Advanced Interpretation Models vol. 3*, 2002.
- [16] A. A. Boughrara, "Injection/Falloff Testing of Vertical and Horizontal Wells," PhD, Petroleum Engineering, University of Tulsa, Tulsa, Oklahoma, U.S.A, 2007.
- [17] M. Li, Q. Li, G. Bi, and J. Lin, "A Two-Phase Flow Model for Pressure Transient Analysis of water Injection Well Considering Water Imbibition in Natural Fractured Reservoirs," *Mathematical Problems in engineering*, 2018.
- [18] A. D. Habte and M. Onur, "Laplace - Transform Finite Difference and Quasistationary Solution Method for Water Injection / Falloff Test," *SPE Journal*, vol. 19, pp. 398-409, 2013.
- [19] S. E. Buckley and M. C. Leverett, "Mechanism of Fluid Displacement in Sands," presented at 1941 New York meeting, 1941.
- [20] A. Kantzas, J. Bryan, and S. Taheri, "Fundamentals of fluid flow in porous media," *Pore size distribution*, 2012.
- [21] U. Taura, P. Mahzari, M. Sohrabi, and S. A. Farzaneh, "A New Methodology for Improved Estimation of Two-Phase Relative Permeability Functions for Heavy Oil Displacement Involving Compositional Effects and Instability," in *SPE Heavy Oil Conference and Exhibition*, 2016.
- [22] B. Kayode, "Accuracy of water break-through time prediction," ed: Google Patents, 2019.
- [23] P. Bhardwaj, R. Manchanda, J. Hwang, P. Cardiff, and M. Sharma, "A New Reservoir Scale Model for Fracture Propagation and Stress Reorientation in Injection Wells," in *50th US Rock Mechanics/Geomechanics Symposium*, 2016.
- [24] W. T. Hauss, "A Numerical Simulation Study on the Characteristics of a Variable Wellbore Storage Pressure Transient Response," *Master of Science, Petroleum engineering*, Texas Tech University, 1988.
- [25] Y. Li, X. Li, S. Teng, F. Wang, and D. Xu, "A new changing wellbore storage model for pressure oscillation in pressure buildup test," *Journal of Natural Gas Science and Engineering*, vol. 19, pp. 350-357, 2014.
- [26] H. Stehfest, "Algorithm 368: Numerical inversion of Laplace transforms [D5]," *Communications of the ACM*, vol. 13, pp. 47-49, 1970.
- [27] A. Bouaffane and K. Talbi, "Thermal study of fluid flow inside an annular pipe filled with porous media under local thermal non-equilibrium condition," *Journal of Mechanical Engineering and Sciences*, vol. 13, pp. 4880-4897, 2019.
- [28] F. H. Escobar, J. M. Navarrete, and H. D. Losada, "Evaluation of pressure derivative algorithms for well-test analysis," in *SPE International Thermal Operations and Heavy Oil Symposium and Western Regional Meeting*, 2004.

- [29] F. H. E. Macualo, E. R. Borrego, and N. T. A. Olaya, "Analysis of Pressure And Pressure Derivative Interference Tests Under Linear And Spherical Flow Conditions," *Revista DYNA*, vol. 85, 2018.
- [30] D. Bourdet, J. Ayoub, and Y. Pirard, "Use of Pressure Derivative in Well Test Interpretation," *SPE Formation Evaluation*, vol. 4, pp. 293-302, 1989.
- [31] S. GeoQuest, "Eclipse technical description manual," ed: Schlumberger Geo-Quest, Houston, TX, 2001.
- [32] J. R. Fanchi, "Principles of Applied Reservoir Simulation," ed: Gulf Professional Publishing, 2018.
- [33] T. T. Mohd, N. A. Bakar, N. Awang, and A. Talib, "Aqueous foams stabilized with silica nanoparticle and alpha olefin sulfonates surfactant," *Journal of Mechanical Engineering and Sciences*, vol. 12, pp. 3759-3770, 2018.
- [34] A. U. Chaudhry, "Oil Well Testing Handbook," Advanced TWPSOM Petroleum Systems, Inc. Houston, Texas, 2004.
- [35] B. Guo, K. Sun, and A. Ghalambor, *Well productivity handbook*: Elsevier, 2014.
- [36] A. Satter and G. M. Iqbal, *Reservoir Engineering: The fundamentals, simulation, and management of conventional and unconventional recoveries*: Gulf Professional Publishing, 2015.
- [37] (11 January, 2020). Fekete Reference Materials: General Concepts; Reservoir Fluid Properties. Available: http://www.fekete.com/SAN/WebHelp/FeketeHarmony/Harmony_WebHelp/Content/HTML_Files/Reference_Material/General_Concepts/Reservoir_Fluid_Properties.htm
- [38] C. H. Whitson and M. R. Brulé, *Phase behavior*: Henry L. Doherty Memorial Fund of AIME, Society of Petroleum Engineers, 2000.
- [39] M. M. Salehi, P. Omidvar, and F. Naeimi, "Salinity of injection water and its impact on oil recovery absolute permeability, residual oil saturation, interfacial tension and capillary pressure," *Egyptian journal of petroleum*, vol. 26, pp. 301-312, 2017.
- [40] A. Bahadori, *Fluid phase behavior for conventional and unconventional oil and gas reservoirs*: Gulf Professional Publishing, 2016.
- [41] H. Zhuang, *Dynamic well testing in petroleum exploration and development*: Newnes, 2012.
- [42] M. A. Al-Marhoun, "The Oil Compressibility below Bubble Point Pressure Revisited-Formulations and Estimations," in *SPE Middle East Oil and Gas Show and Conference*, 2009.
- [43] "The Effect of Wellbore Storage on Surface Data," 2012.
- [44] M. Y. Alklich, B. Ghosh, and E. W. Al-Shalabi, "Tight Reservoir Stimulation for Improved Water Injection-A Novel Technique," in *IPTC 2014: International Petroleum Technology Conference*, 2014.
- [45] W. Ziyi, "Study on the change of porosity and permeability of sandstone reservoir after water flooding," *IOSR Journal of Engineering (IOSRJEN)*, vol. 06, pp. 35-40, 2016.
- [46] T. Ahmed and P. McKinney, *Advanced reservoir engineering– 4th Edition*: Elsevier, 2011.
- [47] D. McClatchie, T. Garner, and J. Yurkanin, "Injection well stimulation: putting away more for less in California waterfloods," in *SPE Annual Technical Conference and Exhibition*, 2004.
- [48] Z. Wu and H. Liu, "Investigation of hot-water flooding after steam injection to improve oil recovery in thin heavy-oil reservoir," *Journal of Petroleum Exploration and Production Technology*, vol. 9, pp. 1547-1554, 2019.